Statistics of self-avoiding walks on randomly diluted lattices

M. D. Rintoul, Jangnyeol Moon,* and Hisao Nakanishi
Department of Physics, Purdue University, West Lafayette, Indiana 47907
(Received 5 November 1993)

A comprehensive numerical study of self-avoiding walks on randomly diluted lattices in two and three dimensions is carried out. The critical exponents ν and χ are calculated for various different occupation probabilities, disorder configuration ensembles, and walk weighting schemes. These results are analyzed and compared with those previously available. Various subtleties in the calculation and definition of these exponents are discussed. Precise numerical values are given for these exponents in most cases, and many new properties are recognized for them.

PACS number(s): 05.40.+j, 05.50.+q, 64.60.Fr

I. INTRODUCTION

In the past decade, the problem of the critical behavior of a polymer [1–3] in a disordered medium has generated a great deal of interest [4–18]. There are many different physical realizations which can lead to such a problem. These include polymers trapped in a porous medium, gel electrophoresis, and size exclusion chromatography, which deal with the transport of polymers through membranes with very small pores.

One of the simplest theoretical models of this problem is that of a self-avoiding walk (SAW) on a percolation cluster. The SAW incorporates many of the important characteristics of the polymer, such as its flexible chain behavior and short distance repulsion, while the percolation cluster represents the random medium. Various analytical methods have been used to attack this problem, such as mean field theories [13,19,20] and different types of renormalization group calculations [4,12,13,21]. Unfortunately there has not been universal agreement among them, due to the difficulty in including the geometrical effect of self-avoidance on a disordered medium.

Because of the difficulties in approaching the problem analytically, there has been extensive computational work done in an attempt to get a precise numerical estimate for many of the quantities which characterize the SAW. Despite the fact that these numerical calculations seem to represent a less complicated, more "brute force" approach to the problem, they too have many subtleties. This has led to a large volume of research with significantly different results for seemingly very similar problems [11,12,14,15,17,18,22]. In this paper, we present a comprehensive numerical study of this controversial problem with a particular focus on the two critical exponents, ν and χ (defined below).

A SAW is usually defined as a random walk which can never intersect itself. On a discrete lattice, the walk is constrained to move to a nearest neighbor site during each time step, where the self-avoidance condition further constrains the walk to occupy only sites which have not been previously occupied. The resulting random process now depends in a complicated way on the history of the walk. Because of this, the formulas which govern the asymptotic behavior of the SAW's are significantly different from those which govern those of free random walks.

Written in terms of the quenched average, the asymptotic behavior for the average mean-square end-to-end distance of a chain on a percolation cluster becomes

$$\overline{\langle {R_N}^2 \rangle} = \frac{\sum_{\mathcal{C}} P(\mathcal{C}) \langle {R_N}^2 \rangle_{\mathcal{C}}}{\sum_{\mathcal{C}} P(\mathcal{C})} \sim N^{2\nu}, \tag{1}$$

where the angular brackets indicate the average over all walks from a given point on a given disorder configuration, and the overbar indicates averaging over disorder. For the latter average, $\mathcal{C}$ represents a disorder configuration, and $P(\mathcal{C})$ is the probability for that configuration to occur. For the sake of specificity, we define $\mathcal{C}$ relative to the fixed starting point of the SAW's.

Similarly, one also expects to be able to write the expression for the average number of walks on the percolation cluster as

$$\overline{Z_N} = \frac{\sum_{\mathcal{C}} P(\mathcal{C}) Z_N(\mathcal{C})}{\sum_{\mathcal{C}} P(\mathcal{C})} \sim N^{\gamma-1} \mu^N. \tag{2}$$

For the full lattice ($p = 1$), this form is known to be consistent with renormalization group and other theoretical studies and with numerical calculations of various types [2]. The value of γ for the full lattice is 43/32 [23] in two dimensions and $\approx$ 7/6 [24] in three dimensions. Note, however, that for the case of $p < 1$, Z_N is a random variable with a multiplicative character so that its mean and most probable values are far apart [14]. This makes it intrinsically rather difficult to extract its true mean. Moreover, under certain conditions on the distribution of $\ln Z_N$ [25], this form itself may have to be replaced by another asymptotic behavior which has a stretched expo-

*Present address: Third Military Academy, Gogyung-Myeon, Yeongchun-kun, Kyungpook 771-840, Republic of Korea.

nential correction term rather than the power law form $N^{\gamma-1}$.

The quenched average defined here is often referred to as *one end fixed* [13] even though the final configurational average eventually accounts for all possible starting points; this is because one end of the SAW's *is* fixed on a given disorder configuration and the final disorder average would not be expected to change the qualitative features of the average from any one *infinite* disorder configuration. Such an average may be related to a polymer solution in a disordered space with one end grafted to (or trapped in) a particular part of the substrate. This situation should generally lead to a stretched conformation since SAW's with the free end in a dense region would dominate the average entropically where such regions are further away from the fixed end than if density did not matter.

Another important exponent which is related to the disorder in the system and has no full lattice analog is χ, which is defined by the fluctuations in the log of the number of walks as follows [13]:

$$\mathrm{var}[\ln Z_N] = \overline{(\ln Z_N)^2} - (\overline{\ln Z_N})^2 \sim N^{2\chi} . \qquad (3)$$

Recently, Le Doussal and Machta [13] proposed the existence of a new disorder fixed point for $p_c < p < 1$ based on renormalization group arguments. The existence of such a regime would be characterized by a change in the value of χ for $p_c < p < 1$ from its value at p_c as well in the value of ν at p_c from the corresponding values at $p = 1$ and $p_c < p < 1$. Initial studies which were performed to look for this crossover have not been fully consistent [13,17].

The aim of this work is to provide a comprehensive study of the two critical exponents ν and χ. The behaviors of the mean-square end-to-end distance and the variance in $\ln Z_N$ are examined for the exponents ν and χ at different occupation probabilities to obtain values both at the critical percolation threshold and in the region where $p_c < p < 1$. Averages over all clusters and the *infinite* cluster are both calculated in order to look for differences between the two. A standard chain averaging and a kinetically weighted average are both used to calculate the exponents. This allows a comparison between different physical processes and also allows previous simulation results to be put in proper perspective. The exponent γ was not analyzed in this work mainly because of the intrinsic difficulties involved in extracting an average from a multiplicative random variable Z_N. A full analysis of the distribution of Z_N and the form of $\overline{Z_N}$ will be left for a future study.

The organization of this paper is as follows. In the next section, we provide a brief summary of the numerical methods used in this work. The enumeration data we have obtained are summarized and the exponent estimates given in Sec. III classified by the exponent and by the type of weighting (see below). In Sec. IV we give detailed comparisons of our new estimates with the other available results and discuss their significance in relation to the previously controversial aspects of this problem. Finally, we draw some conclusions in Sec. V, clarifying the current status of this problem.

II. NUMERICAL METHOD

In this section, we briefly describe the numerical approach we have used in this work. Our approach consists of two parts: we first randomly generated the percolation disorder configurations by Monte Carlo simulation on grids of prescribed sizes. Then SAW's were generated by complete enumeration on each disorder sample. Below we give some details of these two operations.

While much of the computation was performed on standard sequential computers, in those cases where the required CPU time per cluster was small but the required number of clusters was very large, we have resorted to massively parallel computation using a network of 64 Sun workstations. This was done through a prototype parallel toolkit called EcliPSe [26]. Some details of this aspect are given in the Appendix.

A. Generation of percolation clusters

In this work, the percolation clusters were generated using site percolation on the square and simple cubic lattice of edge length L. Different values of L were used for both two and three dimensions in order to test finite size effects. For the bulk of the data that did not deal with finite size effects, the largest convenient value of L was used. In two dimensions, a value of $L = 1000$ was normally used, with the computer memory being the main constraining factor. In three dimensions, L was taken to be 30 mainly due to the constraints imposed by the way we define the infinite cluster.

To construct a cluster, each site on the lattice was assigned to be occupied with probability p. As usual, occupied nearest neighbor sites are connected together and the resulting connected components of the lattice are called *clusters*. Cluster connectivity was determined using a breadth first search algorithm. This was done by going through the lattice and looking for sites that were not already marked as belonging to a given cluster. When such a site was found, the entire cluster was *burned* [27] from that site and a unique label was assigned to the elements in that cluster.

If an *infinite* cluster needs to be identified, the largest cluster is searched for and checked to see whether or not it wraps around the lattice in all directions when periodic boundary conditions are applied. If it does not, it is rejected and a new disordered lattice is constructed. Otherwise, it is accepted. The wrapping requirement was used for two reasons. First, it is a commonly used way to obtain a model for an infinite cluster on a finite system. Also, from a more practical standpoint, the wrapping condition allows us to implement periodic boundary conditions in all directions and, therefore, to choose the starting points for the walks without having to worry about the lattice boundaries. If the given simulation is concerned with all clusters, then all of the clusters are used with periodic boundary conditions.

B. Generation of walks

In the case of all cluster (AC) statistics, starting points for the SAW's were chosen randomly from the entire lat-

tice, with each cluster being effectively weighted by the number of points in the cluster. For infinite cluster (IC) statistics, the points were chosen at random from the *infinite* cluster. Only one starting point was chosen per lattice in this case. This was done to prevent unexpected correlations among the samples which would occur if different starting points were too close to each other. *All* walks less than or equal to a given N were then exactly enumerated. The value of N differed depending on the other parameters of the calculation. It was important to have N as large as possible in order to extract the asymptotic behavior, but not so large that the enumerations would take an unreasonably large amount of time to complete nor that the size of the SAW becomes comparable to the lattice size. Thus the values of N ranged from 25 to 30.

All walks from a given starting point were completely enumerated using a very simple recursive procedure. After an initial site was chosen, a routine was used that marked that site as occupied and attempted to walk to all unoccupied nearest neighbors. If an unoccupied nearest neighbor site was found, the same routine was again used with that new site. This happened until the walk had reached its maximum length or could not find any available sites. If this occurred, the current site was marked as unoccupied and the walk retreated to its previous step and continued to look for different available sites. This method was used to do all of the walk enumeration.

Two types of averaging were used. The first type of averaging used was *chain* averaging. In this method, each walk from a given starting point was given the same weight as every other walk of the same number of steps from that same starting point. This method is the one used in most enumerations and best represents the model on which most theoretical calculations are based. In a polymer solution in random media, it would also represent the case where the chain conformations are in equilibrium with the environment.

The other type of averaging used was a kinetically weighted averaging (previously called *walk* averaging [28]). This average weights the contribution of a given walk to a given measured quantity (such as $\overline{\langle R^2 \rangle}$) based on the inverse of the connectivity of the sites in the walk. Thus, the weight w_{Γ_N} for a given N-step walk Γ_N can be written as

$$w_{\Gamma_N} = \frac{1}{z_0} \prod_{j \in \Gamma_N} \frac{1}{z_j - 1}, \tag{4}$$

where z_j is the connectivity of site j and the product is over all sites except for the origin of the walk. The factor of $z_j - 1$ for $j > 0$ reflects the exclusion of the site that the walk has just left. The chain averaging is just equivalent to setting $w = C_N^{-1}$ for all walks. The *kinetic* average emulates the weighting of a standard Monte Carlo sampling method as applied to a diluted space [11] . It may be described as a kinetic, growing walk (somewhat like the myopic ant) except that it dies upon encountering its own track. The kinetic averages tend to have fewer fluctuations than the chain average for similar samples. In a polymer application, the kinetic averaging may crudely correspond to the case where the chain is being grown *in situ*.

Physically, the chain ensemble appears to be the appropriate one to represent a dilute solution of polymer chains in porous media in *equilibrium*. However, the corresponding free walk problem showed interesting differences between the walk and chain averages [29]. The investigation of possible differences for SAW's appears warranted for this reason, as well as for a proper comparison with some of the previous Monte Carlo results [11].

In order to extract the asymptotic exponent, the effective slope of the plot of $\ln \overline{\langle R^2 \rangle}$ vs $\ln N$ was extracted and plotted against $1/N$. In the case of ν, we have used the effective exponent ν_N as given by the formula

$$2\nu_N = \frac{N \overline{\langle R_N^2 \rangle}}{\frac{1}{2}[\overline{\langle R_1^2 \rangle} + \overline{\langle R_N^2 \rangle}] + \sum_{i=2}^{N-1} \overline{\langle R_i^2 \rangle}} - 1. \tag{5}$$

The effective exponent χ_N was extracted in a similar way, using $\mathrm{var}[\ln Z_N]$. Plotted in this way, the asymptotic value of the exponent should be obtained as $N \to \infty$, or as $1/N \to 0$. The data is presented in this manner in order to better observe the asymptotic behavior of the slope. This also allows us to estimate the error obtained in the extrapolation of the slope to its $N = \infty$ value.

III. RESULTS OF COMPLETE ENUMERATION

In this section, we describe the summaries of the data and the exponent estimates obtained by analyzing them. Detailed discussions on their significance are presented in a separate section following the current one. The final exponent estimates are also given in Tables I and II for the *chain* average and in Tables III and IV for the *kinetic* average.

A. Chain average results for ν

In $d = 2$, data were collected at $p = 0.59273 \cong p_c$ for 6260 independent *infinite* clusters, which were divided into three different runs. These data are shown in Fig. 1. The graph corresponds to the effective slope plot that was described earlier. This slope rises gradually from 0.750 to 0.770 and then appears to level off to give an asymptotic value of $\nu = 0.770 \pm 0.005$. This general trend of rising up and leveling off was seen in each of the three batches separately. The behavior in the case of the all cluster average also gave an exponent estimate of 0.770 ± 0.005 and showed a similar increasing behavior for larger N. These data were taken from 14530 independent disorder realizations. Typical error bars are included for each different set of data in Fig. 1 and the following graphs of the effective value of ν as a function of N. These error bars for the effective slope are calculated directly from the errors in the end to end distance calculation by propagating these errors through Eq. (5). The errors given for the values of the exponents here and elsewhere were estimated by using the scatter in the effective slope graphs for the overall data as well as by considering the batch-

TABLE I. Estimates of critical exponents ν and χ for *chain* averaging for the square lattice in two dimensions. The data for p_c were collected at $p = 0.59273$.

p	$p = p_c$ (IC)	$p = p_c$ (AC)	$p = 0.65 > p_c$ (IC)
ν	0.770 ± 0.005	0.770 ± 0.005	0.770 ± 0.010
χ	0.50 ± 0.01	0.53 ± 0.01	0.47 ± 0.01

TABLE II. Estimates of ν and χ for the *chain* averaging for the simple cubic lattice in three dimensions. The data for p_c were collected at $p = 0.3117$.

p	$p = p_c$ (IC)	$p = p_c$ (AC)	$p = 0.4 > p_c$ (IC)
ν	0.660 ± 0.005	0.645 ± 0.005	0.650 ± 0.005
χ	0.49 ± 0.01	0.55 ± 0.01	0.27 ± 0.01

TABLE III. Estimates of critical exponents ν and χ for *kinetic* averaging for the square lattice in two dimensions. The data for p_c were collected at $p = 0.59273$.

p	$p = p_c$ (IC)	$p = p_c$ (AC)	$p = 0.65 > p_c$ (IC)
ν	0.760 ± 0.005	0.755 ± 0.005	0.750 ± 0.005
χ	0.48 ± 0.02	0.63 ± 0.03	0.30 ± 0.03

TABLE IV. Estimates of ν and χ for *kinetic* averaging for the simple cubic lattice in three dimensions. The data for p_c were collected at $p = 0.3117$. χ for $p = 0.4$ suggested a possibly nonpower law behavior.

p	$p = p_c$ (IC)	$p = p_c$ (AC)	$p = 0.4 > p_c$ (IC)
ν	0.645 ± 0.005	0.625 ± 0.005	0.625 ± 0.005
χ	0.51 ± 0.02	0.66 ± 0.02	

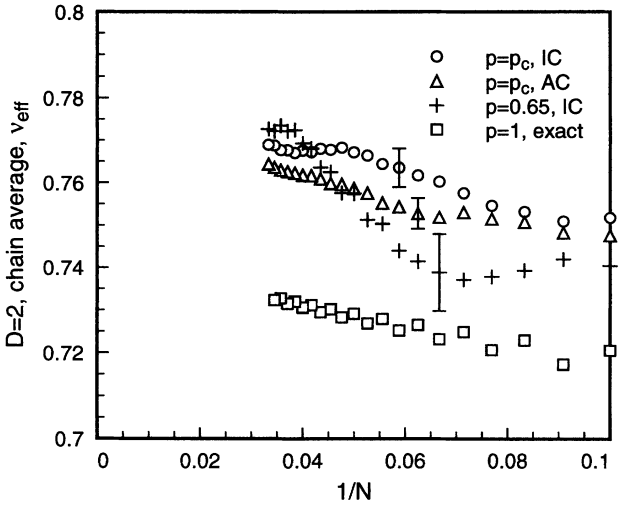

FIG. 1. Effective slope plot of $\overline{\langle R_N{}^2 \rangle}$ for the *chain* averages on $d = 2$ percolation clusters. In the figure, the symbols ○, △, and + denote $p = p_c$ for IC, $p = p_c$ for AC, and $p = 0.65$ for IC, respectively. The symbol □ corresponds to the value of the effective slope as given by Eq. (5) for the full lattice. All full lattice values are from N. Madras and G. Slade, *The Self-Avoiding Walk* (Birkhauser, Boston, 1993).

to-batch fluctuations in the effective slope graphs of the individual batches.

For the case of $p = 0.65 > p_c$, the picture is similar to the $p = p_c$ case. Because of the CPU time constraint involved in enumerating a much larger number of walks than the $p = p_c$ case, we were forced to use fewer starting points. This was not a major setback since moving away from the critical probability caused the fluctuations between averages over different starting points to be smaller. These data (also shown in Fig. 1) seem to point to a value of 0.770 ± 0.005 for ν. The all cluster average is not expected to be significantly different from the infinite cluster average for $p > p_c$, since the infinite cluster overwhelmingly dominates for $p > p_c$.

In the case of $d = 3$ percolating clusters, we first took $p = 0.3117 \cong p_c$ and again performed calculations for both the *infinite* cluster and for all clusters. In both cases, the clusters were constructed on a simple cubic lattice, where $L = 30$. The average was taken over 47 830 independent realizations for the case of all clusters, and 20 000 clusters for the infinite cluster case. The resulting graphs for the effective value of $\overline{\langle R^2 \rangle}$ are shown in Fig. 2. Both graphs are relatively straight, and the asymptotic values of their slopes seem to differ. A careful inspection of the graphs show that $\nu = 0.660 \pm 0.005$ for the IC case, and $\nu = 0.645 \pm 0.005$ for the AC case. The values of the slopes seem to differ more for larger N, which seems to imply that most of the longer walks in the all cluster case are walks which are trapped in isolated clusters (i.e., *not* in the *infinite* cluster).

For $p = 0.4 > p_c$, we also measured ν. This was done only on the *infinite* cluster, but again, for p this large the result should not differ significantly from the all cluster result. Again, the disorder configuration was constructed on a $L = 30$ cubic lattice. However, due to the increased

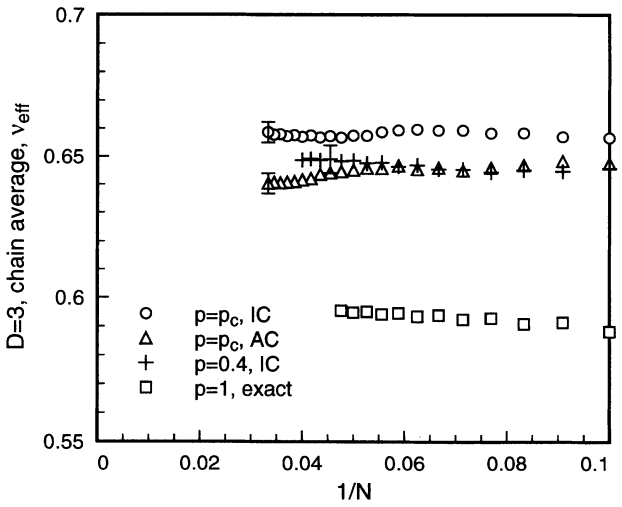

FIG. 2. Effective slope plot of $\overline{\langle R_N{}^2 \rangle}$ for the *chain* averages on $d = 3$ percolation clusters. In the figure, the symbols ○, △, and + denote $p = p_c$ for IC, $p = p_c$ for AC, and $p = 0.4$ for IC, respectively. The symbol □ corresponds to the value of the effective slope as given by Eq. (5) for the full lattice.

density and the greater number of walks, only 3920 clusters were used with $N \leq 25$. The graph of the effective value of 2ν is shown in Fig. 2. The graph is very straight, and shows an asymptotic value of 0.650 ± 0.005 for ν.

B. Kinetic average results for ν

For all of the different types of disorder, the data obtained using the kinetic average showed fewer statistical fluctuations in two dimensions than their chain averaged counterparts. The extrapolated value for ν was slightly different between the two averages. For the IC case, we obtained an asymptotic value of 0.760 ± 0.005 for ν, slightly smaller than the chain average case. The AC average was almost identical to the IC case with a value of 0.755 ± 0.005, which was again smaller than the chain average case. Finally, the $p = 0.65$ case gave a value which was practically indistinguishable from 3/4. The effective slope graphs which led to all three results are shown in Fig. 3.

The case for $d = 3$ is slightly harder to interpret, due to the steady downward trend in the effective value of the exponent for the different cases. To extract the asymptotic value of the slope, we also looked at the radius of gyration average for the same data. In the asymptotic limit, the average of the radius of gyration should have the same slope as the mean-square end-to-end distance. The effective slope generated from this data approached its asymptotic value from below and thus gives an effective bound for the $N = \infty$ value (see also Ref. [14]).

Using the method described above, the value of ν on the infinite percolating cluster was found to be $\nu = 0.645 \pm 0.005$. In the case of all clusters at $p = p_c$, we calculated ν to be 0.625 ± 0.005. For $p = 0.4 > p_c$, the data also seemed to show an asymptotic value of $\nu = 0.625 \pm 0.005$. Like the two dimensional case, the exponent data for the kinetic averages are all lower than their respective chain averages. These data are shown in Fig. 4.

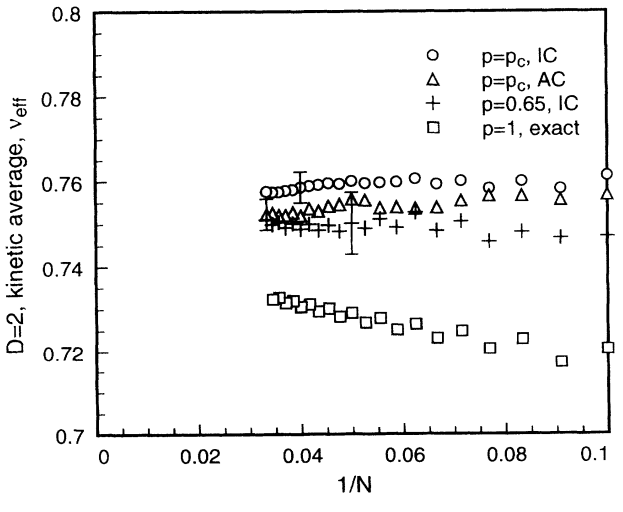

FIG. 3. Effective slope plot of $\overline{\langle R_N{}^2 \rangle}$ for the *kinetic* averages on $d = 2$ percolation clusters. In the figure, the symbols ○, △, and + denote $p = p_c$ for IC, $p = p_c$ for AC, and $p = 0.65$ for IC, respectively. The symbol □ corresponds to the value of the effective slope as given by Eq. (5) for the full lattice.

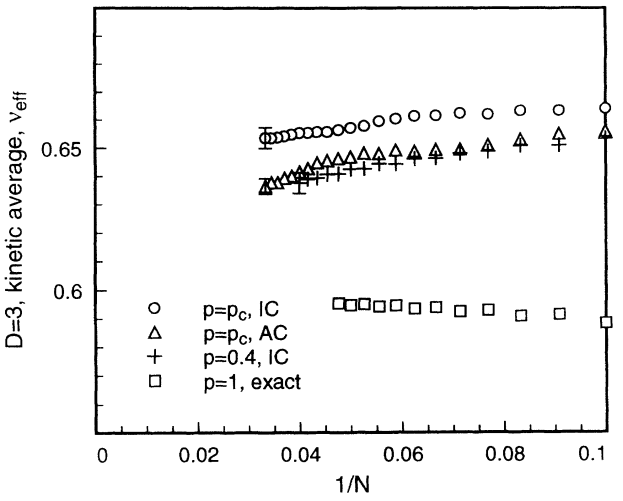

FIG. 4. Effective slope plot of $\overline{\langle R_N{}^2 \rangle}$ for the *kinetic* averages on $d = 3$ percolation clusters. In the figure, the symbols ○, △, and + denote $p = p_c$ for IC, $p = p_c$ for AC, and $p = 0.4$ for IC, respectively. The symbol □ corresponds to the value of the effective slope as given by Eq. (5) for the full lattice.

C. Chain average results for χ

Our data for χ for $p = p_c$ and $d = 2$ are taken from the same calculations as for ν for the case of the *infinite* cluster. These data are shown in Fig. 5. For this case, our estimate of χ is about 0.50 ± 0.01, which is consistent with a value of 1/2. In the case of the all cluster average, the

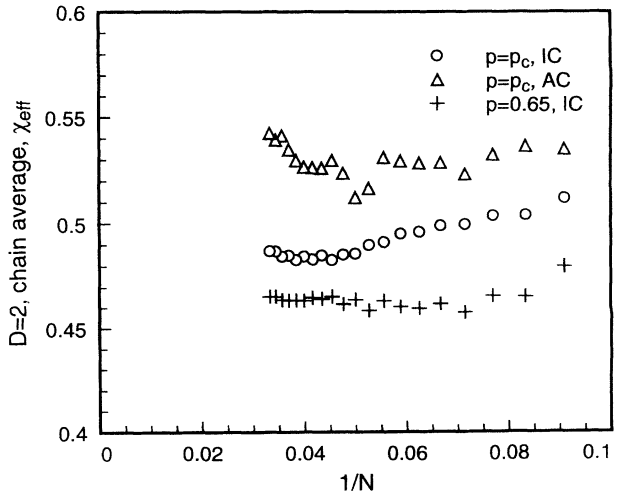

FIG. 5. Effective slope plot of χ for the *chain* averages on $d = 2$ percolation clusters. In the figure, the symbols ○, △, and + denote $p = p_c$ for IC, $p = p_c$ for AC, and $p = 0.65$ for IC, respectively.

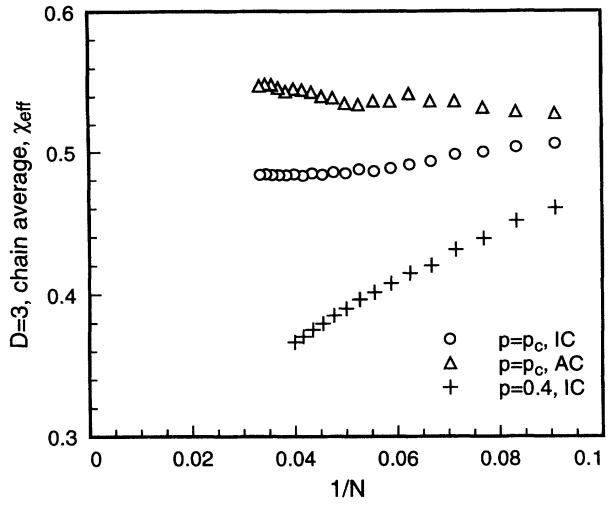

FIG. 6. Effective slope plot of χ for the *chain* averages on $d = 3$ percolation clusters. In the figure, the symbols ○, △, and + denote $p = p_c$ for IC, $p = p_c$ for AC, and $p = 0.4$ for IC, respectively.

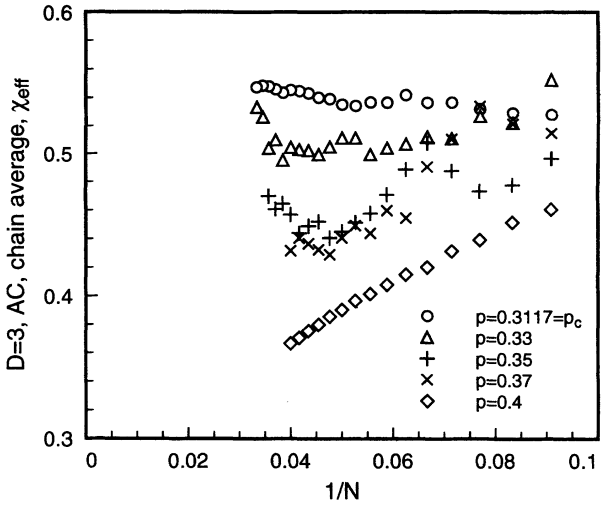

FIG. 8. Effective slope plot of χ for AC *chain* averages on $d = 3$ percolation clusters for various occupation probabilities p. Different symbols correspond to $p = 0.3117$ (○), $p = 0.33$ (△), $p = 0.35$ (+), $p = 0.37$ (×), and $p = 0.4$ (◇).

data are taken from a set that included 10 000 disorder realizations with $N = 25$ steps for the SAW's. It was necessary to take a larger sample of shorter walks in order to reduce statistical fluctuations. The data for all clusters may well point to a slightly larger value for χ. Our best estimate in this case is $\chi = 0.53 \pm 0.01$. The data shown in Fig. 5 seem to strongly suggest that the IC and AC averages are not the same.

The $p = 0.65$ case in two dimensions in Fig. 5 shows a significantly different result than the $p = p_c$ case. The data points to a value of 0.47 ± 0.01 for χ. These data exhibit very little statistical fluctuations and constitute strong evidence for a new disorder behavior for $p > p_c$, different from both that for p_c or the pure lattice behavior.

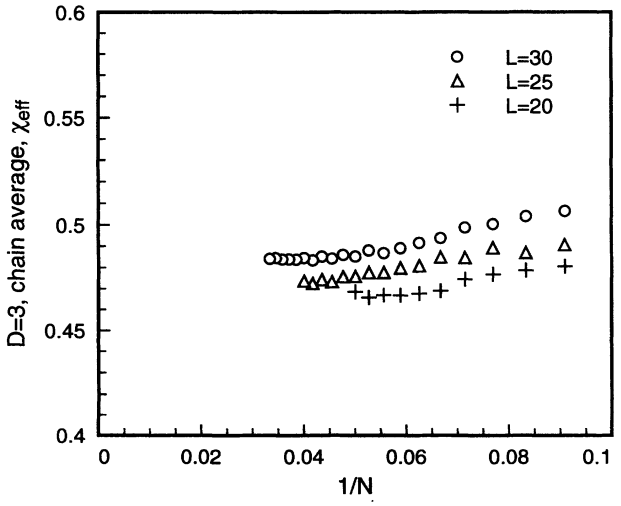

FIG. 7. Effective slope plot of χ for *chain* averages on $d = 3$ percolation clusters at $p = p_c$ on simple cubic lattices of various size. Different symbols correspond to $L = 30$ (○), $L = 25$ (△), and $L = 20$ (+).

In three dimensions, we calculated χ using the same data sets as were used in the calculation of ν. These data are shown in Fig. 6. The graph for the all cluster average is fairly straight and yields a value of $\chi = 0.55 \pm 0.01$ in this case. The exponent in the infinite cluster case is harder to extract since there seems to be a downward trend in both the $p = p_c$ and $p = 0.4$ case. If these slopes are linearly extrapolated out to their $N = \infty$ limit, one gets a value of $\chi = 0.49 \pm 0.01$ for the $p = p_c$ case and $\chi = 0.27 \pm 0.02$ for the $p = 0.4$ case. We believe, however, that this downward trend for large N in the IC case may be due to finite size effects for the case of $p = p_c$. To show this, we extracted the effective slope of χ for *infinite* clusters built on simple cubic lattices of size $L = 20$ and $L = 25$ to compare with the $L = 30$ case. All three cases are shown in Fig. 7. This graph explicitly shows the increasingly downward behavior of χ for decreasing lattice size.

The downward trend in χ for $p = 0.4$ is much sharper, and significantly different from the $p = p_c$ case. In order to check whether this was the asymptotic value for χ for all $p_c > p > 1$, we also collected exact enumeration data for various p, where $p_c \leq p \leq 0.4$. These results (shown in Fig. 8) apparently indicate that the asymptotic value of χ decreases with increasing occupation probability p. This could even imply that the asymptotic behavior of χ for $p > p_c$ does not follow a power law.

D. Kinetic average results for χ

A corresponding definition of χ for kinetic averaging can be given by

$$\mathrm{var}[\ln w_N] = \overline{(\ln w_N)^2} - (\overline{\ln w_N})^2 \sim N^{2\chi}, \qquad (6)$$

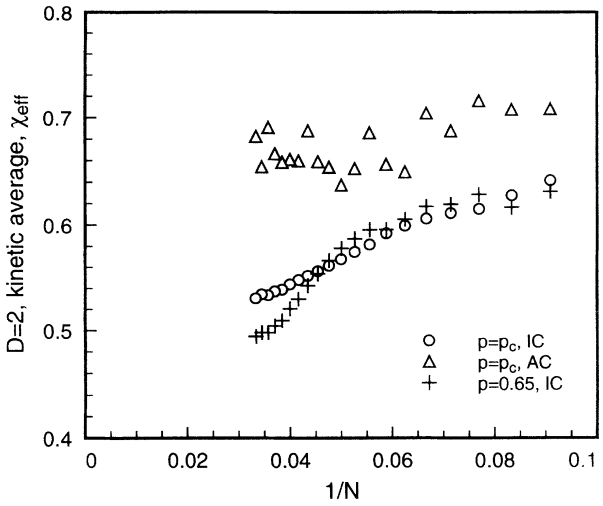

FIG. 9. Effective slope plot of χ for the *kinetic* averages on $d = 2$ percolation clusters. In the figure, the symbols ○, △, and + denote $p = p_c$ for IC, $p = p_c$ for AC, and $p = 0.65$ for IC, respectively.

where w_N is the total remaining weight of all of the N step walks originating from a given starting point. Thus, the *kinetic* χ is defined by the variance of the log of the total amount of weight associated with each walk. Although the amount of weight starts out with a value of 1, weight can be lost at each step if the walk is *completely* trapped by the medium (and cannot grow) or if it intersects itself. This is different from the chain average where weight is effectively lost any time a vacant site is encountered during the chain enumeration.

The data for χ at p_c in two dimensions for the kinetic average is shown in Fig. 9. The IC average for $p = p_c$ can be extrapolated to get a value of 0.48 ± 0.02. Since the graph seems to be leveling off, a value $1/2$ is certainly not excluded. Like the chain average, the AC exponent is larger, but in the kinetic average the difference between the IC and AC cases is much larger. The AC average points to an asymptotic value of 0.63 ± 0.03. The asymptotic value for χ when $p = 0.65 > p_c$ seems to be falling off very rapidly towards a value of 0.30 ± 0.03, but it is possible that it could be continuing down even farther.

In three dimensions, the effective slope graph for the kinetically averaged χ is even more similar to the chain averaged χ, but the difference between the IC and AC case is again more pronounced. The AC case seems to be approaching a value of 0.66 ± 0.02, while the IC value is approaching a value of 0.51 ± 0.02. Like the chain averaged χ, the two- and three-dimensional results show qualitatively very similar behavior for $p > p_c$. The exponent χ for $p > p_c$ seems to be rapidly approaching a value of zero, which may suggest a behavior that is not a power law for at least some values of $p > p_c$. These data are shown in Fig. 10.

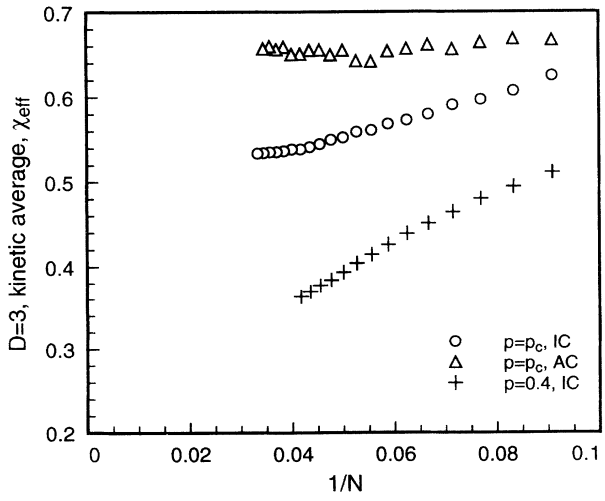

FIG. 10. Effective slope plot of χ for the *kinetic* averages on $d = 3$ percolation clusters. In the figure, the symbols ○, △, and + denote $p = p_c$ for IC, $p = p_c$ for AC, and $p = 0.4$ for IC, respectively.

IV. DISCUSSION

In this section, we present a detailed comparison of our enumeration results with other available estimates and discuss the new findings in the broader perspective. Unfortunately there seem to be no analytical calculations which provide the relevant exponent estimates with any reasonable level of accuracy. Therefore, we first give detailed discussions of the available numerical results, and at the end offer comparisons with some theoretical predictions such as mean field and scaling arguments, and certain renormalization group calculations.

A. Exponent ν for the infinite cluster (IC) average at $p = p_c$

Our present estimates of $\nu = 0.770 \pm 0.005$ in $d = 2$ and $\nu = 0.660 \pm 0.005$ in $d = 3$ for the chains on the infinite cluster at $p = p_c$ represent a refinement of the values that were proposed in several other works recently. Our values are expected to be much more precise than earlier estimates due to the fact that *all* walks from a given starting point are enumerated, and the number of disorder configurations chosen was very large. This precision is best seen by the fact that it passes the very stringent criterion of having the plot of the effective slope as a function of the number of steps show very little statistical fluctuation. Vanderzande and Komoda [17] obtained the result $\nu = 0.77 \pm 0.01$ for chains on the IC using the exact enumeration method. They defined their infinite cluster as a cluster which *spanned* the entire lattice, as opposed to our condition that it *wrapped* in every dimension. We tried both types of requirements for our IC results and found little difference between them. The wrapping condition was chosen for our results since it allowed us to use periodic boundary conditions and to choose our starting point anywhere inside the cluster. Infinite clusters defined by the wrapping condition were also used in Ref. [14] for the three-dimensional case. They obtained a value of 0.65 ± 0.01 for ν.

Many previous IC results were obtained using in whole or in part a Monte Carlo simulation. Among them, the work of Ref. [11] arrived at the conclusion that the asymptotic estimate of ν changed very little by lattice dilution, even at the critical dilution. These simulations were performed on wrapping clusters as in this work but with *kinetic* averaging. Thus, we postpone the discussion on those results toward the end of this subsection where we focus on the kinetic averaging.

Some of the other previous works for IC configurations were performed using a different type of *infinite* cluster. In this situation the infinite cluster was chosen based on a predetermined maximum chemical distance from a seed site chosen on the cluster. For some of these enumerations, the clusters were grown with the standard Leath algorithm [30]. This algorithm starts with a seed site and grows the cluster in shells around that site. If any configuration that contains at least one walk (no single isolated sites) is accepted, and walks are enumerated from the seed, the resulting average is an AC average. However, if the configurations are only accepted after growing a certain chemical distance M, then the clusters were considered *infinite* clusters. This method has an advantage in that there are no boundary conditions to consider, and in some cases is more computationally efficient than generating random numbers for the occupation at each site of a large hypercubic lattice. However, it does have problems. The choice of M which defines the IC is not as directly related to the length scale of the cluster as L is when clusters are generated on a periodic lattice.

This type of IC was recently used by Grassberger [18] to obtain results for ν in two dimensions. For this simulation, he chose only those clusters with a chemical distance > 200. This Monte Carlo simulation was different than most previous ones because it first evaluated the average connectivity of the cluster, and then chose the sampling probability based on that. For ν on the IC in two dimensions, he calculated a value of 0.786 ± 0.003. This number was obtained by taking walks up to a maximum of 100 steps [and using $O(10^4)$ different configurations to average over disorder]. However, even for N this large, the average number of walks per sample was approximately 5000. Although the method Grassberger used to obtain this value certainly should be sound, it seems unlikely that such a small error bar could be assigned from a simulation that used so few walks per disorder sample.

It is interesting to note that the kinetic average results on the infinite cluster indicate a somewhat smaller ν than the chain averaged results. The difference between the two cases is small, but appears to be significant. To understand why the kinetic average gives a smaller exponent, it is important to note the main difference between the two averages. In the kinetic average, an N step walk α will carry with it a certain weight, w_α, relative to the rest of the N step walks. All of the $N + M$ step walks which originate from α will have a total weight of w_α, minus the weight of the walks lost due to collisions and trapping. In the chain average, however, the relative weighting of all of the $N + M$ step walks will depend on the total number of $N + M$ step walks.

Now consider a walk which leaves a very highly connected part of the cluster, such as the backbone, and moves on to a dangling end. This walk, and all of the longer walks that it generates, will be trapped on this dangling end, and won't be able to travel very far. In the chain average, these walks will not carry much of the weight since many more walks will be generated on the highly connected part of the cluster. However, in the kinetic average, these walks will still contribute total weight equal to the weight of the original walk, until they eventually begin to die out after getting trapped. Because of this, these trapped walks will contribute a much larger contribution to the total average while they are alive. Since the dangling ends occur on all length scales, there will always be these contributions which keep the kinetic exponent lower.

A seemingly puzzling fact is that, for most values of N considered in this paper, the actual average end-to-end distance of the walks in the kinetic average is larger than those from the chain averaging [14]. This is because, for these values of N, the walks on the dangling ends (which are more spread out and less compact than the rest of the cluster) contribute a larger end-to-end distance towards the average than the chains on the dangling ends. However, when these walks on the dangling ends die out due to trapping, their contribution towards the kinetic average is lost much faster than the contribution to the chain average. The net result is a larger increase in $\langle R^2 \rangle$ for the chains and therefore a larger ν. This, of course, means that, eventually for much larger N, the value of $\langle R^2 \rangle$ must be larger for the chain averaging.

We tested this idea by performing the same two averages with the walks constrained to move on the *backbone* of the infinite cluster. The backbone was defined as the multiply connected part of the *infinite* cluster defined previously, when periodic boundary conditions were applied. Since the dangling ends are now removed, the walk and chain averages should be approximately the same. As seen in Fig. 11, both graphs are almost exactly the same for large values of N, and are both extrapolated to a value of $\nu = 0.775 \pm 0.005$. This result is very similar to that of Woo and Lee [31] which quoted a value of 0.77 ± 0.01 for ν on the backbone of the *infinite* cluster on the square lattice.

We now return to the discussion of Ref. [11]. These simulations were carried out with statistical weights as in our *kinetic* averaging. However, their results obviously do not agree with the present calculation for the IC average at $p = p_c$. A careful analysis of those data in fact suggests that they were not representative of the true average properties of the walk. The main reason that the exponent for the diluted case appeared to be the same as the full lattice is believed to be as follows: The specific Monte Carlo method that was used attempted a fixed number of walks from each starting point. For large N, most of these walks died out on the diluted lattices. If all of the walks died out on a lattice for a given N, then it was not counted in the ensemble average. Unfortunately, there were so few walks (on the order of several hundred) attempted from each starting point that only the starting points which happened to be on the very dense parts of the IC survived to contribute for large N. In other

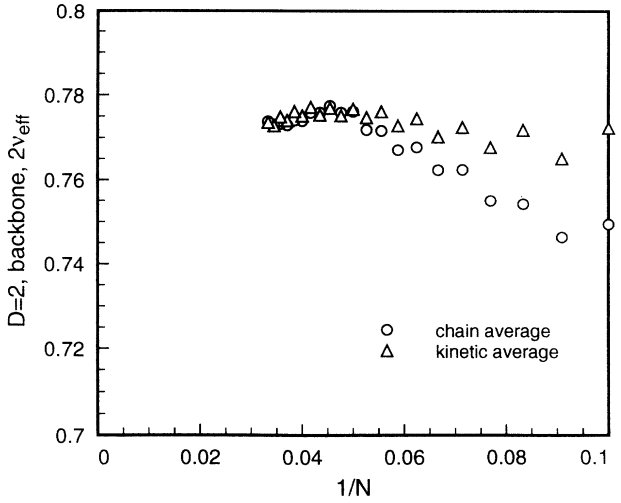

FIG. 11. Effective slope plot of $\overline{\langle {R_N}^2 \rangle}$ for *kinetic* and *chain* averages on the backbone of $d = 2$ percolation clusters at $p = p_c$. In the figure, the symbols ○ and △ denote *chain* and *kinetic* averages, respectively.

words, starting points in sparse regions were systematically excluded from the averaging process. Because of this, the results were biased toward the dense clusters, and therefore the ν that was measured was too small.

We have verified this scenario by performing simulations under the same condition as in Ref. [11], and found that if more walks are attempted from each starting point, a value of ν more consistent with the enumeration results is obtained. In fact, the number of attempted walks from each starting point in Ref. [11] corresponds roughly to that for which on average only one walk would survive the attrition at about the number of steps N where those early simulations reported a downward (or leveling) trend for their estimates of the effective exponent ν_N. We also verified that having a large number of starting points per cluster did not significantly affect the results.

B. Exponent ν for all cluster (AC) average at $p = p_c$

The AC value of ν at $p = p_c$ has perhaps been the most studied and most debated of all of the quantities discussed in this paper. Our estimate of 0.770 ± 0.005 in two dimensions shows that the value of ν is definitely larger than the full lattice value of 0.75. Besides the data shown in Fig. 1, we also performed many enumerations which used slightly smaller maximum lengths but many more disorder configurations. These runs also gave an asymptotic value of 0.770 for ν in the AC case, and showed no fluctuations that could possibly point to a value at or lower than 0.75.

There were also previous enumeration works [14] performed to determine ν in two and three dimensions. In those works, the clusters were generated using the shell method described earlier, requiring each disorder configuration to have at least 200 shells in two dimensions. Averaging over 1000 different disorder configurations, a value of $\nu = 0.78 \pm 0.01$ was obtained. Although the requirement that the clusters have at least 200 shells causes the result to lie somewhere between the AC and IC cases, this result is still a useful one since both ensembles give approximately the same answer. In Ref. [18] Grassberger obtained a value of 0.785 ± 0.003 for ν in the AC, $p = p_c$ case, based on his incomplete enumeration. While our analysis does show that there could still possibly be some upward trend in the estimates of ν, we do not believe that its value would be quite as large as in Ref. [18].

These works seemed to settle the question of whether or not the value of ν in two dimensions increases from the full lattice value to the case of critical dilution. However, there have been a few recent works that still put the value for ν in the AC case to be possibly equal to that of the fully occupied lattice. In Ref. [17], Vanderzande and Komoda estimated a value of $\nu = 0.745 \pm 0.010$. Although this was an exact enumeration performed in a way almost identical to our own, their value was significantly lower. This is possibly due to the fact that they did not attempt to extract the asymptotic value of the slope. For smaller N the value of the slope is less than 0.75, so a least-squares fit to the data that included these small N values could possibly yield a number that low. Woo and Lee [31] also gave a value of approximately 0.75 for the AC average. This is probably related to the fact that they used a Monte Carlo method with weighting more similar to a kinetic average than to a chain average. To test this, we attempted a similar simulation with the same parameters as Ref. [31] and also obtained a value of $\nu = 0.75$.

In three dimensions, the differences between the AC and IC averages at $p = p_c$ are much more significant than the $d = 2$ case. As stated earlier, this is probably due to the fact that the IC makes up a much smaller fraction of the disorder configuration, and most walks find themselves trapped on smaller isolated clusters. Reference [14] obtained an estimate of $\nu = 0.65 \pm 0.01$ by an enumeration of 5200 different clusters. These clusters were grown with the shell method and required to have at least 95 shells. Vanderzande and Komoda [17] also studied the $d = 3$ case with the enumeration method and got a value of 0.635 ± 0.010 for the AC case, which is compatible with our value within the error bars. Unlike their result in two dimensions, we would expect their estimate in three dimensions to be close to ours even though they do not try to extrapolate their value out to $N = \infty$. This is due to the fact that the effective exponent in the $d = 2$ case has an upward trend for larger N, while the effective exponent in the $d = 3$ case remains relatively constant for all N.

A different sort of exact enumeration was recently reported by Smailer *et al.* [32] to extract ν for a continuous disorder instead of a discrete disorder as in percolation. This means that the space is not divided into regions of different, discrete statistical weights (or equivalently *energy* cost) as in percolation (where accessible sites have zero energy and the inaccessible sites have infinite energy barrier), but each site or point in space is associated with a continuously varying *energy* cost of hosting a

part of the chain. The basic assumption in this work appears to be that the finite temperature asymptotic properties of the SAW in a quenched, continuously random environment are governed by the zero temperature fixed point, and that the properties of this latter fixed point would correspond to the discrete percolation disorder at $p > p_c$. They then calculate the zero temperature properties in the continuous disorder problem by looking at the minimum energy SAW by complete enumeration. More specifically, they considered the minimum energy SAW of length N (where $N \leq 20$) in a square and simple cubic lattices where the lattice sites were assigned energies based on a given distribution, and then averaged the properties of the minimum energy walks over many ($\sim 10^5$) disorder configurations. In two dimensions, two different energy distributions were studied. For a Gaussian distribution with mean 0 and variance 1, a value of $\nu = 0.81 \pm 0.02$ was obtained, while a uniform distribution of energies between 0 and 1 gave a value of $\nu = 0.80 \pm 0.02$. In three dimensions, just the uniform distribution was studied and a value of $\nu = 0.71 \pm 0.03$ was calculated.

Although in their work [32] they compared the exponent estimates they obtained with other, previous estimates for the percolation disorder *at* $p = p_c$, they should be properly compared with the percolation results for $p > p_c$. In any case, these values, especially the value in three dimensions, seem to be much larger than those obtained for the percolation disorder results for $p = p_c$ (this work as well as Refs. [14] and [17]), and also more than those for $p > p_c$ from our present calculations (see below).

C. Exponent ν for $p > p_c$

The result for $p = 0.65 > p_c$ in $d = 2$ is also very interesting. While most previous works indicated that many of the asymptotic properties of the SAW in the $p_c < p < 1$ regime should be the same as for $p = 1$, our data seem to indicate otherwise. This was also true with the data from Ref. [18], although Grassberger again obtained a number which is significantly larger than ours (0.815 ± 0.005). The data from Ref. [17], however, gave a value of 0.75 ± 0.01 for this case. This is somewhat lower than our value and happens to be equal to the value for $p = 1$. We note that Ref. [17] stated that only a few hundred different starting points were used for large p. Even though the fluctuation is generally less for $p > p_c$ and a smaller sample space would give adequate results, for data in batches of that size we certainly observed fluctuations large enough to account for the difference. In addition, this difference could also be partly due to the fact that the slope was not extrapolated, as we discussed about their data for the $p = p_c$ case.

Like the $d = 2$ case, the value of ν for $p = 0.4 > p_c$ in three dimensions was definitely not equal to the full lattice value, but was found to equal 0.650 ± 0.010. This is also very similar to the value of 0.645 ± 0.010 reported in Ref. [17].

D. Exponent χ for $p = p_c$ and $p > p_c$

The values of χ obtained for the $p = p_c$ cases are important because they represent a quantity which could be used to distinguish between the IC and AC cases. In both two and three dimensions, the AC exponent is clearly larger than the IC exponent. This is one of the best instances of an exponent which gives a clear numerical difference between these two cases. Since the significance of χ was mentioned only recently [13], there have been few numerical studies done to measure it. Vanderzande and Komoda calculated χ in Ref. [17], but instead of using var[$\ln Z_N$], they used var[$\ln(Z_N + 1)$] [33]. Although the difference between these quantities is small, it may be sufficient to affect the estimate of χ. In fact, it is easy to show that the leading order difference between these two terms is

$$2 \langle \ln(Z_N) \rangle \left\langle \frac{1}{Z_N} \right\rangle . \tag{7}$$

This term is very small for large Z_N, but for small values of N it can be significant. This point is illustrated in Fig. 12. Because of this, their data points for small N are displaced downward and the fitted value of the slope is biased toward a greater value. Their estimates for the AC case of χ in two and three dimensions at $p = p_c$ were 0.65 ± 0.02 and 0.64 ± 0.02, respectively, in contrast to our much smaller estimates (cf. Table II). When we used the same quantities, var[$\ln(Z_N)$] to test this idea, we obtained graphs and resulting exponent estimates quite similar to theirs.

Also, the behavior of χ for $p > p_c$ was examined. The values that we obtained for the specific values of p ($p = 0.65$ in $d = 2$ and $p = 0.4$ in $d = 3$) were much lower than for $p = p_c$, possibly indicating a new disorder fixed point for $p_c < p < 1$. Our estimates appear to be consistent with those given in Ref. [17], (0.43 for $p = 0.65$ in $d = 2$ and 0.33 for $p = 0.4$ in $d = 3$) although no error bars

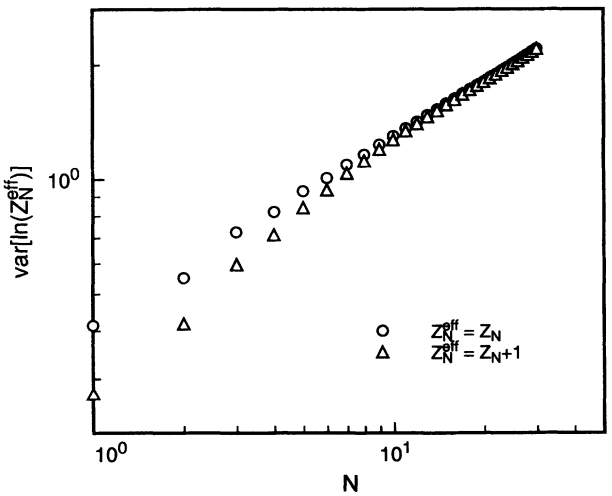

FIG. 12. Plot of var[$\ln(Z_N^{\text{eff}})$] vs N, where the symbol ○ corresponds to $Z_N^{\text{eff}} \equiv Z_N$ (our method) and the symbol △ corresponds to $Z_N^{\text{eff}} \equiv Z_N + 1$ (as in Ref. [17]).

were given in their results. We do not expect there to be a problem with the fact that they were measuring $\ln(Z_N + 1)$ in this case since they explicitly stated that they extracted χ from their data for larger N. Although it is very clear that χ indicates a different behavior for $p > p_c$ than for $p = p_c$, it is *not* at all clear that there was a similar behavior for all $p_c < p < 1$. We note that for larger p, it even seemed possible that var$[\ln Z_N]$ did not follow a power law behavior.

Finally we looked at χ for kinetically averaged walks in a disordered medium. This average describes walks that would be formed if they were *grown* in the medium. The behavior of χ for these kinetically averaged walks displayed the same qualitative behavior as those walks which were averaged according to the chain statistics. However, the difference in χ at p_c for the AC and IC cases was much more pronounced in the kinetic case.

Values of χ were also calculated by Smailer *et. al.* in Ref. [32]. They obtained a value of 0.28 ± 0.03 for χ in two dimensions and 0.15 ± 0.03 in three dimensions. As previously mentioned, these values probably correspond more to the $p > p_c$ values than to the $p = p_c$ values. These values are considerably smaller than the values we have measured using the chain averaging for $p > p_c$. However, they are somewhat similar to the values we obtain using kinetic averaging.

E. Comparison with theoretical predictions

So far, we have only discussed available numerical estimates in comparison with our current results. Here we will give a short discussion of the comparison of our numerical results with the analytically obtained estimates. This discussion is only meant as a numerical comparison and the reader is referred to the original works for the theoretical arguments which led to the numbers we discuss.

In Ref. [13], Le Doussal and Machta used real space renormalization, field theoretic renormalization, and Flory type mean field arguments to study this problem. As for the field theoretic studies, they concluded that the previous study [12] was incorrect and that their own work was inconclusive and that more work was called for. On the other hand, their real space renormalization group study used hierarchical lattices to numerically estimate the value of ν and χ on percolation clusters. Their numerical estimates were significantly different than the ones obtained here for percolation clusters on Euclidean lattices. For ν (referred to as ζ in Ref. [13]) at $p = p_c$, they obtained a value of 0.850, and for $p_c < p < 1$, they find $\nu = 0.862$. Although no direct claim was made as to what percolation system their model corresponded to, the hierarchical lattice used was the one they referred to as a *two-dimensional* model. However, there seems to be no way to reconcile these numbers with the ones we obtained and other numerical estimates available in the literature. Even their full lattice value of 0.847 does not seem to fit in with any usual percolation system. Their estimate of χ for that same system was 0.48 at $p = p_c$ and 0.29 for $p_c < p < 1$, again much different from the values we find (noting, particularly for p_c, that their results are more closely interpreted as the AC ensemble results). However, the prediction that the variation of ν between $p = 1$ and $p_c < p < 1$ is about 2% is not too far from what we find (2.7%), although we disagree with their prediction that ν at p_c is within 1% of its value for the full lattice. In short, their real space renormalization results do not agree with our present ones quantitatively although there are some qualitative agreements.

The same paper also provides various mean field arguments to derive expressions for ν and χ in terms of d and ν_0, the pure lattice value for ν. These expressions were derived with no consideration for the *critical* disorder, and thus should presumably correspond to the case $p_c < p < 1$ at best.

The first set of expressions they obtain are

$$\nu_1(d) = \frac{1}{1 + d(1 - \nu_0)/2}, \tag{8}$$

$$\chi_1(d) = \nu_1(1 - d\nu_0/2) = \frac{1 - d\nu_0/2}{1 + d(1 - \nu_0)/2}. \tag{9}$$

These expressions [13] follow from the known scaling behavior [34] of the probability distribution for the size of the pure SAW in the *stretched* region and dimensional analysis. The first formula gives values of 0.8 and 0.618 for ν_1 in two and three dimensions, respectively. These values are not very far from those we obtained, especially in two dimensions. However, the values for χ_1 is 0.2 in two dimensions and drops to 0.07 in three dimensions. These values of χ_1 do not correspond well to our estimates either for $p_c < p < 1$ or at $p = p_c$.

Their alternative Flory arguments led to several other possible expressions. For example, by expanding on the idea that the disorder introduces an effectively attractive interaction among the *replicas* (when the problem is formulated using the *replica* technique [35]), they obtain

$$\chi_2 = \frac{2 - d\nu_0}{3 - d\nu_0}. \tag{10}$$

This expression gives the values of 1/3 for two dimensions and 0.19 for three dimensions. Again this prediction is quantitatively not very good; however, the decreasing trend of χ for increasing dimension (for $p_c < p < 1$) does appear to be given correctly. Yet another Flory expression they provide is

$$\nu_3 = \nu_0, \tag{11}$$

$$\chi_3 = 1 - d\nu_0/2. \tag{12}$$

This set of expressions follow from a Flory argument where the effect of random environment is treated only dimensionally. The predicted values are again not quantitatively acceptable for any value of p.

Obukhov [19] proposed a relation between χ and ν,

$$\chi = 2\nu - 1. \tag{13}$$

This result would follow if one assumed that the fluctuation N^χ in $\ln Z_N$ were accounted for by the stretching entropy of the form R^2/N. Like the relations proposed

in Ref. [13], this expression would apply for $p_c < p < 1$ and not for $p = p_c$, if at all. Indeed, our numerical values are in reasonably good agreement with this relation for $p > p_c$, but not for $p = p_c$. It is interesting to note that the goodness of this relation may suggest that the effect of self-avoidance is only to rescale R and the fundamental relation between R and the fluctuation in $\ln Z_N$ remains unaffected (at least for $p_c < p < 1$).

While most of the above discussions in fact concerns $p > p_c$, there exist also a large number of Flory type predictions for the exponent ν at p_c in the literature (but so far not for χ). Most of these arguments use the fractal dimension d_f of the critical percolation cluster or that of the backbone, d_f^B to take account of the underlying geometry. This seems to imply that they are all specifically for the IC ensemble and *not* for AC. (Note, however, that Ref. [10] discussed the relationship between the exponent ν in the two ensembles and Ref. [36] which argued that they are the same.) Simplest of these mean field expressions is

$$\nu = \frac{3}{2 + d_f}, \tag{14}$$

which follows by substituting d_f for the Euclidean dimension d in the corresponding full lattice Flory expression [6]. Somewhat ironically, this turns out to yield a very good numerical agreement, giving 0.77 for two dimensions and 0.66 for three dimensions.

Many of the more complicated predictions, all of which arise from some form of mean field approximation, were summarized in a brief paper by Kim [37]. Roughly, there are two types of such approximations; in one type, different formulas follow because of the different postulated forms of the entropic contribution to the Flory free energy, while in the other type, the argument is based on the dimer formation of two SAW's. In both cases, the possibility of using either the full fractal dimensionality d_f or the backbone fractal dimensionality d_f^B effectively doubles the number of different predictions. There are far too many formulas to reproduce here and their predicted values for ν at p_c range from about 0.71 to 0.78 in two dimensions and from 0.61 to 0.66 in three dimensions, the variation being partly due to the uncertainties in the fractal dimensionalities needed to evaluate the formulas.

The most notable feature of these Flory predictions is that they all produce reasonable numerical predictions and, since there is no reason in general to expect a Flory prediction to be *exact*, we cannot rule out any of them simply because of a slightly worse agreement with the numerical results. This means that we cannot at this time rule in favor of or against the respective assumptions in the form of the entropic term in the free energy which resulted in different Flory formulas. It is, however, ironic that the most simple minded Flory approximation Eq. (14) gives the best and almost exact agreement with our results. This might mean that the effect of critical disorder is mainly to affect the scaling behavior of the interaction term and the form of the entropic contribution largely remains unaffected. Such a scenario cannot be entirely correct, however, for it could not possibly explain the results for $p > p_c$.

V. CONCLUSIONS

Having performed a large scale complete enumeration work and having made detailed comparisons with other available estimations of the relevant exponents, we would like to offer some concluding remarks.

We believe that, this work, along with some other recent works, definitely rules out the possibility that the value of ν for critically disordered media is unchanged from its full lattice value in two and three dimensions. In both cases, the value is distinctly larger. We even find very strong evidence that the value of ν is increased from the full lattice value for p significantly above the percolation threshold. We also find very strong evidence that the kinetic averaging gives a slightly lower value of ν for some cases of disorder due to probability trapping, and present numerical data to verify this explanation. Also, the results of previous Monte Carlo simulation [11] which gave incorrect results are explained.

The exponent χ was also studied in great detail, and many previously unknown properties were recognized. The values of χ on the infinite cluster and on all clusters are significantly different. This is one of the clearest examples of a critical exponent giving different results for these two ensembles. Also, our initial numerical studies of χ suggest that its behavior may not be the same for all $p_c < p < 1$, and the variance of $\ln Z_N$ may not even follow a power law in this regime. However, definite conclusions on this point cannot be drawn from the present work alone and must await further investigation.

With regard to the status of theoretical understanding, it seems appropriate to say that currently there exists *no* theory that is quantitatively acceptable as the solution to this problem. This would include real space renormalization, field theoretic renormalization, and various mean field approximations. In particular, there seems to be no good mean field approximation for the exponent χ either at p_c or for $p_c < p < 1$. Many Flory approximations for ν give reasonable predictions for ν, but the simplest possible, uncontrolled approximation happens to give the best agreement. We interpret this as an indication that the basic physics of this problem is still not understood.

ACKNOWLEDGMENTS

This work was supported in part by a grant from ONR. We are grateful to P. Grassberger, S. B. Lee, and J. Machta for fruitful and stimulating discussions, and to C. Vanderzande for clarifying communication. In addition, some of the computations used a parallel toolkit called EcliPSe developed by Rego, Sunderam, and Knop and were carried out with their critical assistance. We are deeply grateful for this help.

APPENDIX: MASSIVELY PARALLEL COMPUTATION

Many of the results described in this paper were obtained on a Kubota Pacific Titan P-3000 mini-

supercomputer. The average CPU time taken for an enumeration with a particular occupation probability and disorder type was about 5000 minutes in total. For some of the higher occupation probabilities, a prototype KPC K-3400 Alpha AXP workstation was used. These platforms are of a standard sequential type. However, for some parts of the enumeration work, we have made use of massively parallel computation over a distributed set of Sun workstations.

Specifically, a massively parallel algorithm was used to generate the data for cases where the average run time per cluster was small, but the number of clusters needed was very large. This was done using a prototype package called EcliPSe [26]. EcliPSe is a library which supports concurrent execution of applications over machines which are connected via a network as well as on parallel hardware such as the Intel iPSC860. In our case, the enumeration task was spread over 64 Sun-4 workstations. These machines were intended primarily for instructional purposes and we were able to take advantage of the school vacation periods when they were largely idle.

Parallelization of the algorithm was performed in collaboration with the developers of the toolkit [38], and was not difficult in technical terms. The task of generating a cluster, choosing a starting point for the walks, and enumerating them was assigned to every machine. As the machines finished their task and reported their results, they were asked to repeat the process. This was done until a preset number of clusters were assigned.

In a practical sense, however, the notion of parallelizing a number of processes whose run times vary greatly presents some problems. This was the case with the enumeration of the walks. Most importantly, one must choose a fixed number of walks and run the enumeration to completion. This can be understood by first looking at the case of running the different batches sequentially. If we stop the enumeration at a random time and reject the enumeration from the current starting point, we are more likely to be rejecting a longer run and are biasing the statistics toward the clusters with fewer walks. Similarly, if we stop the simulation and accept the current starting point we are biasing the results toward the clusters with more walks.

If we now consider a similar situation, but with a large number of processors all working at once, the problem becomes worse as the results from the shorter enumerations pile up very quickly. If we stop all the processes at a random time, and reject all of the enumerations that all of the N processors are working on, we are effectively eliminating the N longest enumerations from the results. Since the distribution is so wide in the case of SAW's on disordered media, this makes the results of a prematurely terminated job useless, unless there are many orders of magnitude more clusters than processors.

Another practical problem which arose from the wide distribution of the number of walks is that of parallelization efficiency. Since some of the enumerations took much longer than others, there was a great deal of dead time at the end of the job as most of the processors were idle while the last few were finishing up. This was a significant problem since the total number of starting points was only a couple of orders of magnitude more than the number of processors. In some cases, the amount of time spent waiting for the last 10 enumerations to finish was as large as the amount of time spent on all of the previous enumerations (≈ 5000). This effect cut our parallelization efficiency from 64 (the total number of processors) effectively to about 30 or 40, depending on the parameters. A way of reducing this effect would be to generate all of the clusters and starting point *first*, and then estimating the number of walks in each case using some sort of Monte Carlo method. Then, the clusters could be ordered with respect to the estimated time that they would take, and the larger ones could be started first.

[1] P. J. Flory, *Statistical Mechanics of Chain Molecules* (Interscience, New York, 1969).

[2] P. G. de Gennes, *Scaling Concepts in Polymer Physics* (Cornell University Press, Ithaca, 1979).

[3] J. des Cloizeaux and G. Jannink, *Polymers in Solution: Their Modeling and Structure* (Oxford, New York, 1990).

[4] B. K. Chakrabarti and J. Kertész, Z. Phys. B **44**, 221 (1981).

[5] B. Derrida, J. Phys. A **14**, L5 (1981).

[6] K. Kremer, Z. Phys. B **45**, 149 (1981).

[7] A. B. Harris, Z. Phys. B **49**, 347 (1983).

[8] J. W. Lyklema and K. Kremer, Z. Phys. B **55**, 41 (1984).

[9] A. K. Roy and B. K. Chakrabarti, Z. Phys. B **55**, 131 (1984).

[10] A. K. Roy and B. K. Chakrabarti, J. Phys. A **20**, 215 (1987).

[11] S. B. Lee and H. Nakanishi, Phys. Rev. Lett. **61**, 2022 (1988); S. B. Lee, H. Nakanishi, and Y. Kim, Phys. Rev. B **39**, 9561 (1989).

[12] Y. Meir and A. B. Harris, Phys. Rev. Lett. **63**, 2819 (1989).

[13] P. L. Doussal and J. Machta, J. Stat. Phys. **64**, 541 (1991).

[14] J. Moon, Ph.D. thesis, Purdue University, 1991; see also H. Nakanishi and J. Moon, Physica A **191**, 309 (1992).

[15] H. Nakanishi and S. B. Lee, J. Phys. A **24**, 1355 (1991).

[16] C. Vanderzande and A. Komoda, Europhys. Lett. **14**, 677 (1991).

[17] C. Vanderzande and A. Komoda, Phys. Rev. A **45**, R5335 (1992).

[18] P. Grassberger, J. Phys. A **26**, 1023 (1993). Note that the estimate of ν for the AC ensemble quoted in this paper has a misprint. The value of 0.783 ± 0.003 appears there but it was meant to be 0.785 ± 0.003 according to its author.

[19] S. P. Obukhov, Phys. Rev. A **42**, 2015 (1990).

[20] A. K. Roy and A. Blumen, J. Stat. Phys. **59**, 1581 (1990).

[21] M. Sahimi, J. Phys. A **17**, L379 (1984).

[22] P. M. Lam, J. Phys. A **23**, L831 (1990).

[23] B. Nienhuis, Phys. Rev. Lett. **49**, 1062 (1982).

[24] See, e.g., D. C. Rappaport, J. Phys. A **18**, 113 (1985).

[25] A. Giacometti and A. Maritan, Phys. Rev. E **49**, 227 (1994).

[26] V. J. Rego and V. S. Sunderam, J. Parallel Distrib. Comput. **14**, 66 (1992); a winning entry for the 1992 Gordon Bell Prize Competition by H. Nakanishi, V. Rego, and

V. Sunderam was the first application of EcliPSe to the problem described in this paper.
[27] H. J. Herrmann, D. C. Hong, and H. E. Stanley, J. Phys. A **17**, L261 (1984).
[28] A. Maritan, Phys. Rev. Lett. **62**, 2845 (1989).
[29] A. Giacometti, H. Nakanishi, A. Maritan, and N. H. Fuchs, J. Phys. A **25**, L461 (1992).
[30] P. L. Leath, Phys. Rev. Lett. **36**, 921 (1976).
[31] K. Y. Woo and S. B. Lee, Phys. Rev. A **44**, 999 (1991).
[32] I. Smailer, J. Machta, and S. Redner, Phys. Rev. E **47**, 262 (1993).
[33] C. Vanderzande (private communication).
[34] S. Havlin and D. Ben Avraham, Adv. Phys. **36**, 155 (1987).
[35] M. J. Stephen and G. S. Grest, Phys. Rev. Lett. **38**, 567 (1977).
[36] Y. Kim, Phys. Rev. A **41**, 4554 (1990).
[37] Y. Kim, Phys. Rev. A **45**, 6103 (1992).
[38] EcliPSe of Ref. [26] was further developed by V. J. Rego and P. Knop at Purdue University (1993).